Inorganic Chemistry

Article

Structure and Vibrational Properties of Oxohalides of Vanadium

Vincent Guiot,[†] Irene Suarez-Martinez,[†] Philipp Wagner,[†] Jonathan Goss,[‡] Patrick Briddon,[‡] Abdul W. Allaf,[§] and Christopher Paul Ewels*,[†]

Institut des Matériaux Jean Rouxel (IMN), Université de Nantes, CNRS, 2 rue de la Houssinière, BP32229, 44322 Nantes, France, School of Electrical, Electronic and Computer Engineering, University of Newcastle, Newcastle Upon Tyne, NE1 7RU, United Kingdom, and Atomic Energy Commission, Department of Chemistry, P.O. Box 6091, Damascus, Syria

We study the structure and vibrational modes of a wide range of oxohalides of vanadium (VOX_nY_m; X, Y = F, Cl, Br, I; $n, m = 0-3$, $n + m \leq 3$). The results agree well with experimental results for $VOCl_3$ and VOF_3 and suggest reassignment of the experimentally observed VOF to VOF_2. We provide new assignments for various experimental modes, identifying several intermediates ($VOBr_2$, VOBr) and mixed structures (e.g., $VOCl_2Br$), and discuss formation trends and stabilities.

1. Introduction

Many high-valence transition metals form oxohalides[1] (also referred to in the literature as oxyhalogenides, oxyhalides, and oxide halides). They are strong oxidizing agents[2] used as reagents in organic synthesis,[3,4] as well as in chemical vapor deposition,[5] and as catalysts in the production of ethylene–propylene rubbers.[6]

Vanadium has catalytic properties that make it useful in many industrial applications. Vanadium pentoxide is used as a catalyst in the production of sulfuric acid and in the manufacturing of maleic anhydride, which is needed to make polyester resin and fiberglass. Vanadium plays an important role in battery technology and rust-resistant and high-speed tool steels, as a bonding agent in cladding titanium to steel, and generally by the aerospace industry in titanium alloys. Also, medical implants often contain vanadium alloys, which contribute to their long life.

Vanadium has four major oxidation states, resulting in a range of oxides: V_2O_5 (+5), VO_2 (+4), V_2O_3 (+3), and VO (+2). The oxohalides of vanadium, VOX_nY_m (X, Y = F, Cl, Br, I; $n, m = 0-3$, $n + m \leq 3$), are generally prepared from the oxides[7] but are not particularly well-known. The former oxidation state (+5), such as VOX_3 and VO_2X where X is a halogen, are relatively stable. The latter vanadium oxohalide compounds (+4), such as VOX_2, are notably hydroscopic and hydrolyze vigorously to the hydrous pentoxide.

Among the oxohalides of vanadium, the oxotrihalides, VOX_3, are the most studied. $VOCl_3$ is commercially available and is often used as a molecular precursor in high-valence vanadium chemistry.[1] For example, $VOCl_3$ can be used to synthesize VOF_3, $VOBr_3$, and VOI_3 by reacting it in the gas phase at high temperatures and low pressures with halogen containing salts such as NaF, KBr, and KI.[8]

Experimental IR spectra are available in the literature for $VOCl_3$,[8-10] VOF_3,[8,7] and $VOBr_3$.[8,11] Due to difficulties in synthesis, there is only one experimental report of VOI_3.[8] Theoretical frequencies have been calculated for $VOCl_3$, VOF_3, $VOBr_3$, and VOI_3.[12]

The only available experimental structural parameters for vanadium oxotrihalides are for $VOCl_3$,[13,14] although calculated values exist for other vanadium oxotrihalide mol-

---

* To whom correspondence should be addressed. E-mail: chris.ewels@cnrs-imn.fr.
† CNRS Nantes Institute of Materials.
‡ University of Newcastle.
§ Atomic Energy Commission.

(1) Greenwood, N. N. Earnshaw, A. *Chemistry of the Elements*, 1st ed.; Butterworth-Heinemann: Oxford, 1989.
(2) Yajima, A.; Matsuzaki, R.; Saeki, Y. *Bull. Chem. Soc. Jpn.* **1978**, *51*, 1098.
(3) Crans, D. C.; Chen, H.; Felty, R. A. *J. Am. Chem. Soc.* **1992**, *114*, 4543.
(4) Meier, I. K.; Schwartz, J. *J. Am. Chem. Soc.* **1989**, *111*, 3069.
(5) Anpo, M.; Sunamoto, M.; Che, M. *J. Phys. Chem.* **1989**, *93*, 1187.

(6) Rawe, A. *Principles of Polymer Chemistry*; Springer: New York, 2000; ISBN 0306463687, p 276.
(7) Selig, H.; Claassen, H. H. *J. Chem. Phys.* **1966**, *44*, 1404.
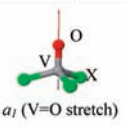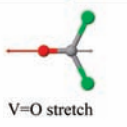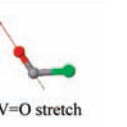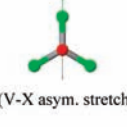(8) Zidan, M.; Allaf, A. *Spectrochim. Acta A* **2000**, *56*, 2693.
(9) Miller, F. A.; Cousins, L. R. *J. Chem. Phys.* **1957**, *26*, 329.
(10) Clark, R. J. H.; Rippon, D. M. *Mol. Phys.* **1974**, *28*, 305.
(11) Miller, F. A.; Baer, W. K. *Spectrochim. Acta A* **1961**, *17*, 112.
(12) Socolsky, C.; Brandan, S. A.; Ben Altabef, A.; Varetti, E. L. *THEOCHEM* **2004**, *45*, 672.
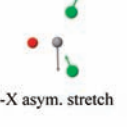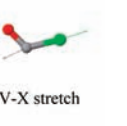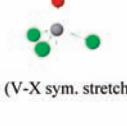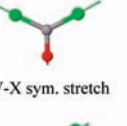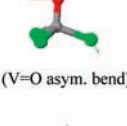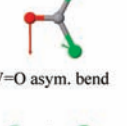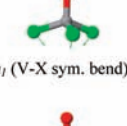
10.1021/ic8022562 CCC: $40.75 © 2009 American Chemical Society
Published on Web 03/23/2009

Table 1. Vibrational Modes of VOX$_3$, VOX$_2$, and VOX, in Order of Decreasing Frequency[a]

VOX$_3$	VOX$_2$	VOX
a_1 (V=O stretch)	V=O stretch	V=O stretch
e (V-X asym. stretch)	V-X asym. stretch	V-X stretch
a_1 (V-X sym. stretch)	V-X sym. stretch	
e (V=O asym. bend)	V=O asym. bend	
a_1 (V-X sym. bend)	V-X sym. bend	
e (V-X asym. bend)	V-X asym. bend	O=V-X bend

[a] The following tables respect the same frequency ordering. Bonds are hidden where necessary to see the modes.

ecules.[12] Increasing the atomic number of X in VOX$_3$ leads to a corresponding increase in the V−X bond length. The VOX$_3$ molecules have C_{3v} symmetry and nine vibrational modes, three of which are doubly degenerate. This results in six vibrational frequencies (Table 1): three strong corresponding to stretching of V=O (symmetric) and V−X (symmetric and asymmetric) and three weaker corresponding to bending of O=V−X (symmetric) and V−X (symmetric and asymmetric).[8,12] Both theory and experimentation confirm a decrease of frequencies with an increasing atomic mass of the halogen. Additional peaks associated with Cl isotopes (^{35}Cl and ^{37}Cl) have also be seen in VOCl$_3$ FTIR spectra.[15]
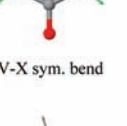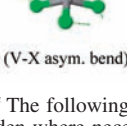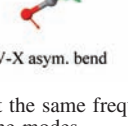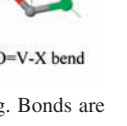
VOCl and VOF have recently been studied by infrared spectroscopy[16,17] and Hartree−Fock and density functional theory (DFT) modeling.[16−18] These molecules can be obtained by passing gas-phase VOCl$_3$ and VOF$_3$ directly over heated silver at high temperatures and low pressures.[16,17] Although calculated frequencies are generally in good agreement with experimental results, there has been difficulty in reproducing the observed V−F stretching frequencies of VOF observed at 807 cm^{-1}.[18] No experimental value for the

low-frequency X−V=O bending mode has been reported directly in the literature.[18] Moreover, theoretical models disagree concerning the value of the angle X−V=O, for which wide variation is observed.[16−18]

VOX molecules belong to the C_s symmetry point group, and exhibit three vibrational frequencies (Table 1) corresponding to V=O stretching, V−X stretching, and X−V=O bending. Structural parameters have been theoretically calculated.[18] To date, there are no reported data for VOX$_2$ nor for mixed species VOX$_n$Y$_m$ (X, Y = F, Cl, Br, I; X ≠ Y; n, m = 1−2, $n + m \leq 3$).

While many experimental spectra show unassigned peaks[8,16,17] and since no systematic theoretical study yet exists, we study here the family VOX$_n$Y$_m$ (X, Y = F, Cl, Br, I; n, m = 0−3, $n + m \leq 3$) to obtain a complete set of structural and vibrational data and propose original assignments of observed peaks.

2. Methods

We use spin-polarized DFT calculations under the local density approximation[19] as implemented in the AIMPRO package.[20,21] The calculations were carried out using large supercells, fitting the charge density to plane waves within an energy cutoff of 300 Ha. Charge density oscillations in partly filled degenerate orbitals during the self-consistency cycle were damped using a Fermi occupation function with $k_B T = 0.04$ eV. Relativistic pseudo-potentials are generated using the Hartwingster−Goedecker−Hutter scheme.[22] Atom-centered Gaussian basis functions are used to construct the many-electron wave function. These functions are labeled by multiple orbital symbols, where each symbol represents a Gaussian function multiplied by polynomial functions including all angular momenta up to maxima p ($l = 0, 1$), d ($l = 0, 1, 2$), and f ($l = 0, 1, 2, 3$). Following this nomenclature, the basis sets used for each atom type were *dddfd* (V), *ppppp* (O), *dddd* (Cl), and *fddd* (Br and I) with increasing functional localization from left to right (a more detailed discussion of the basis functions can be found in ref 23). A Bloch sum of these functions is performed over the lattice vectors to satisfy the periodic boundary conditions of the supercell. While we allowed full spin relaxation, in all cases, VOX molecules were found to be most stable with an effective spin of 1, VOXY with a spin of 1/2, and VOXY$_2$ with no spin (X, Y = F, Cl, Br, I). Since no indication about the symmetry of VOX$_2$ and VOXY was found in the literature, we did not impose symmetry constraints. However, after full geometric optimization, the VOX$_2$ molecules all showed C_{2v} symmetry. The vibrational modes of the species VOX$_n$ ($n = 1,3$) are given in Table 1.

Vibrational frequencies and normal modes are obtained as follows. Each atom in a relaxed molecular structure is displaced in the x, y, and z directions by 0.2 au in turn, and the forces on all atoms are evaluated analytically. The second derivative of the energy with respect to the positions of atoms i and j, $d^2E/dR_i dR_j$, is then obtained by a finite difference formulation of the derivative using the calculated forces. From these numerical second deriva-

(13) Oberhammer, H.; Strähle, J. *Z. Naturforsch. A* **1975**, *30*, 296.
(14) Karakida, K.; Kuchitsu, K. *Inorg. Chim. Acta* **1975**, *13*, 113.
(15) Filgueira, R. R.; Fournier, L. L.; Varetti, E. L. *Spectrochim. Acta A* **1982**, *38*, 965.
(16) Allaf, A. W. *J. Chem. Res.* **2003**, *9* (S), 554.
(17) Allaf, A. W. *J. Chem. Res.* **2003**, *12* (S), 800.
(18) Diez, R. P.; Baran, E. J. *J. Mol. Struct.* **2005**, *732*, 155.

(19) Perdew, J. P.; Wang, Y. *Phys. Rev. B: Condens. Matter Mater. Phys.* **1992**, *45*, 13244.
(20) Jones, R.; Briddon, P. *Semiconductors Semimetals* **1998**, *51A*, 287.
(21) Rayson, M. J.; Briddon, P. R. *Comput. Phys. Commun.* **2007**, *178* (2), 128−134.
(22) Hartwingster, C.; Goedecker, S.; Hutter, J. *Phys. Rev. B: Condens. Matter Mater. Phys.* **1998**, *58*, 3641.
(23) Goss, J. P.; Shaw, M. J.; Briddon, P. R. *Top. Appl. Phys.* **2007**, *104*, 69–94.

Table 2. Structural Parameters for VO$_n$Cl$_m$ (Å for bond lengths and deg for angles)^a

	VOCl$_3$		VOCl$_2$	VOCl		VO$_2$Cl
	present work	literature	present work	present work	literature	present work
V=O	1.59	1.571,[12] 1.57,[14] 1.571[13]	1.59	1.60	1.594,[18] 1.56[16]	1.60
V−Cl	2.11	2.168,[12] 2.142,[14] 2.137[13]	2.12	2.15	2.26,[18] 2.33[16]	2.13
O=V−Cl	108.3	107.8[13]	116.4	120.6	139.1,[18] 179.97[16]	113.6
Cl−V−Cl	110.6	110.9,[12] 111.3,[14] 111[13]	127.2			
O−V−O						108.2

^{a} Experimental data in italics.

Table 3. Calculated and Literature Frequencies for VO$_n$Cl$_m$ (cm^{-1})^a

VOCl$_3$		VOCl$_2$	VOCl		VO$_2$Cl
present work	literature	present work	present work	literature	present work
1046	1043,[12] 1035,[8] 1042.8,[15] 1042.5,[25] 1035[9]	1041	1014	1032.9,[18] 1010[16]	1025
502	503,[12] 505,[8] 508.4,[15] 503,[25] 504[9]	524	427	388.1,[18] 420[16]	1010
397	409,[12] 408,[8] 413.2,[15] 409.5,[25] 408[9]	386			471
243	246,[12] 248,[25] 249,[9] 246[10]	220			346
161	164,[12] 163,[25] 165,[9] 163[10]	116			190
126	125,[12] 124.5,[25] 129,[9] 124.5[10]	32	154	72.9[18]	161

^{a} Experimental data in italics.

tives, the dynamical matrix can be built up by dividing each term by the product of the masses of atoms i and j, $(d^2E/dR_idR_j)/M_iM_j$, and the subsequent eigenvalue problem solved in the usual way.

Although this procedure is derived using a harmonic approximation, the numerical nature of the second derivatives can be viewed as including contributions from quartic and higher-order even terms in the vibrational potential, and as such, the frequencies obtained are termed *quasi-harmonic*. A detailed discussion of this method is given in ref 24.

Where experimental data are available (e.g., for VOCl$_3$), we obtain bending modes typically within 5 cm^{-1}. However, the calculated stretching frequencies, which generally have a larger anharmonic component,[24] are slightly less accurate (errors varying from about 10 to 30 cm^{-1}) with a general correlation of increasing error with increasing frequency. To compensate for this effect, we correct the frequencies obtained from the dynamical matrix by applying a constant shift (considering all cited molecules) of −27 cm^{-1} to all stretching frequencies (i.e., those involving both V−O as well as V−X; X = F, Cl, Br, I). All tabulated values incorporate this global mean shift.

3. Results

3.1. Vanadium Oxochlorides VOCl$_x$. VOCl$_3$ is the most well-characterized of the vanadium oxohalides, and our results are in good agreement with experimental[13,14] and theoretical[12] data from the literature (less than 0.06 Å difference for bond lengths, less than 0.7° difference for angles; see Table 2). Our calculated vibrational frequencies are given in Table 3, and once again show good general agreement with the literature.

(24) Jones, R.; Goss, J.; Ewels, C.; Oberg, S. *Phys. Rev. B: Condens. Matter Mater. Phys.* **1994**, *50*, 8378.
(25) Clark, R. J. H.; Mitchell, P. D. *J. Chem. Soc.* **1972**, *22*, 2429.

Calculations on isotopes of VOCl$_3$ (with ^{35}Cl and ^{37}Cl) show coherent behavior of the vibrational frequencies with increasing atom mass (Table 4). Frequency shifts are proportional to the number of ^{37}Cl atoms in the molecule and do not affect the V=O stretching mode. Agreement with shifts reported by Filgueira et al.[15] is excellent for the symmetrical V−Cl stretching mode, but we see a discrepancy for the asymmetrical V−Cl stretching mode. This can be corrected by inverting the assignments given by Filgueira et al. for the VO^{35}Cl^{35}Cl^{37}Cl and VO^{35}Cl^{37}Cl^{37}Cl isotopes, restoring a more logical frequency sequence with mass.

We consider next VOCl, with structural data given in Table 2. Our calculated structure shows good agreement on bond lengths with calculations in the literature[18] (less than 0.11 Å difference). Our O=V−Cl angle is about 20° less than that of Diez and Baran,[18] and about 40° less than that of Allaf;[16] however, both groups agree that the real value should be smaller than their calculations.[16,18] No experimental values are available. We see excellent agreement between our calculated vibrational frequencies and experimental data (Table 3). Notably, the V−Cl stretch mode matches experimental results[16] better than previous calculations.[18] Our O=V−Cl bend mode is higher than previous calculations[16,18] due to our smaller bond angle (no experimental data are available for comparison).

Our calculated frequencies confirm the experimental attribution of VOCl.[16] Our calculated V=O stretch frequency for VOCl$_2$ is very close to that of VOCl$_3$, and the V−X stretch lies within the broad shoulder of the VOCl$_3$ V−X stretch, which suggests that VOCl$_2$ is probably experimentally undetectable by FTIR without going to higher spectrometer resolutions. It therefore remains possible that dissociation of VOCl$_3$ can also form VOCl$_2$ along with VOCl. Another potential product, VO$_2$Cl, does not have frequencies that match peaks in the experimental spectra. Cl isotopic shifts for VOCl and VOCl$_2$ are given in Table 5, although no experimental data are yet available for comparison.

3.2. Vanadium Oxofluorides VOF$_x$. In this section, we begin by modeling VOF$_3$ for which various theoretical and experimental data are available in the literature and then consider other compounds. We notably discuss the peak attribution in the experimental VOF[17] and VOF$_3$[8] spectra (Figures 1 and 2).

For VOF$_3$, we obtain excellent agreement with theoretical[12] structural data in the literature where available, of less than 0.03 Å difference for bond lengths and less than 0.3° difference for angles (Table 6). Vibrational frequencies are given in Table 7. Stretching modes show good agreement with the literature (variations from 1 to 12 cm^{-1}), and bending modes differ by less than 20 cm^{-1}.

Tables 8 and 9 show new results for the hypothetical intermediate molecules VOCl$_2$F and VOClF$_2$, which could be created when VOCl$_3$ reacts with NaF[8,16,17] to produce VOF$_3$. Compared to VOCl$_3$ or VOF$_3$, these molecules have a lower symmetry which breaks degeneracy and increases the number of frequencies. Their calculated frequencies are often very near to those of VOCl$_3$ and VOF$_3$; in particular,

Table 4. Calculated and Literature Frequencies for VOCl$_3$ with Varying Chlorine Isotopes (cm^{-1})[a]

| VOCl$_3$		^{35}Cl^{35}Cl^{37}Cl		^{35}Cl^{37}Cl^{37}Cl		^{37}Cl^{37}Cl^{37}Cl	
present work	literature	our DFT shift	literature shift	our DFT shift	literature shift	our DFT shift	literature shift
1046	1043,[12] *1035,*[8] *1042.8,*[15] *1042.5,*[25] *1035*[9]	0	*0*[15]	0	*0*[15]	0	*0*[15]
502	503,[12] *505,*[8] *508.4,*[15] *503,*[25] *504*[9]	−2	*−3.73*[15]	−4	*−1.8*[15]	−6	*−5.7*[15]
397	409,[12] *408,*[8] *413.2,*[15] *409.5,*[25] *408*[9]	−3	*−3.22*[15]	−7	*−6.3*[15]	−10	*−9.6*[15]

[a] Experimental data in italics.
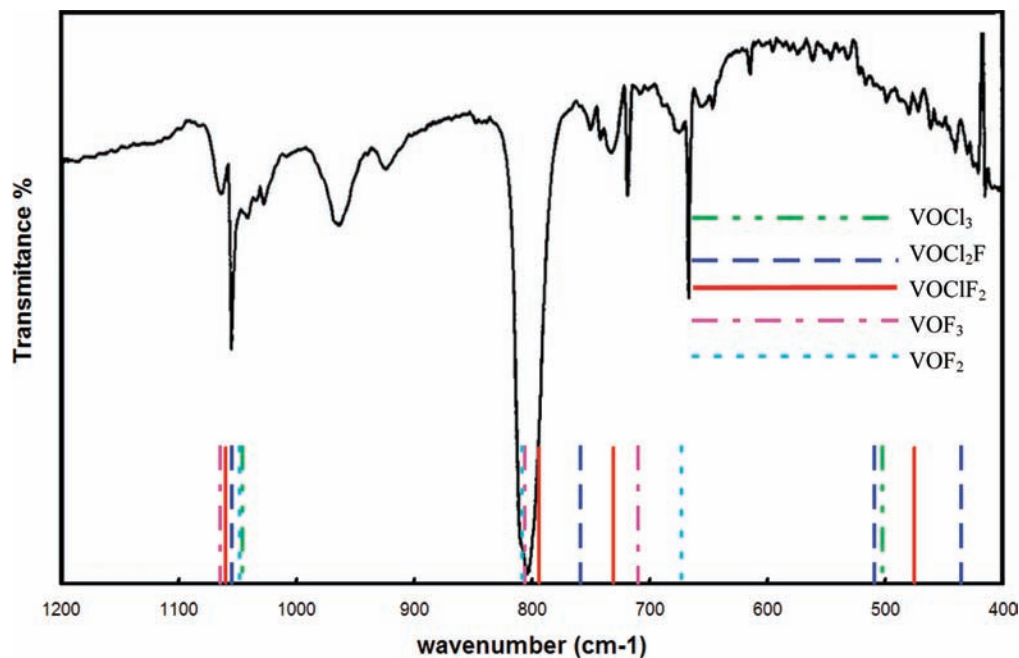
Figure 1. VOF$_3$ FTIR absorption spectrum (cm^{-1}), modified from ref 8. Colored bars correspond to our calculated frequencies for various molecules, as given in the legend. Several previously unassigned peaks are due to VOF$_2$, VOCl$_2$F, and VOClF$_2$.

Table 5. Calculated and Literature Frequencies for VOCl and VOCl$_2$ with Varying Chlorine Isotopes (cm^{-1})[a]

VOCl		VO^{37}Cl	VOCl$_2$	^{35}Cl^{37}Cl	^{37}Cl^{37}Cl
present work	literature	our DFT shift	present work	our DFT shift	our DFT shift
1014	1032.9,[18] *1010*[16]	0	1041	0	0
427	388.1,[18] *420*[16]	−7	524	−3	−6
154	*72.9*[18]	−1	386	−4	−9
			220	−1	−1
			116	−2	−3
			32	0	0

[a] Experimental data in italics.

the experimentally observed shoulders[8] around two of the main peaks of VOF$_3$ (1058 and 722 cm^{-1}) we assign here to VOCl$_2$F and VOClF$_2$ (see Figure 1). Other peaks of these compounds around 500 cm^{-1} are hidden by the noise. The weak peak intensities suggest low concentrations of these intermediates in the gas phase. We note that the P and R sidebands observed in the VOF$_3$ FTIR spectra of ref 7 are too weak to be observed in the current spectra.

We turn next to VOF. As for VOCl, our structural parameters (Table 6) show good agreement on bond lengths with those reported in the literature[17,18] (less than 0.09 Å difference), with O=V−X angles ∼20° less than those in ref 18 and ∼40° less than those in ref 17, apparently closer to experimental results,[17,18] although no experimental data are available. Once again, this results in a higher calculated O=V−F bending mode (Table 7).
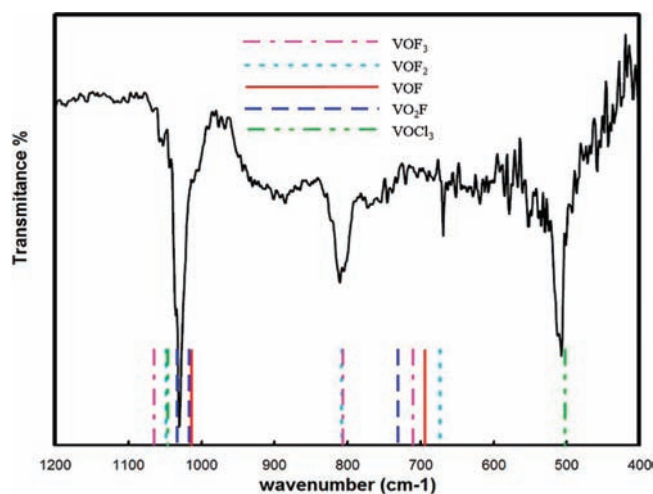
Figure 2. "VOF$_x$," FTIR absorption spectrum previously assigned to VOF, modified from ref 17. Colored bars correspond to our calculated frequencies for various molecules, as given in the legend. Peaks at 668.7, 807, and 1048 cm^{-1} are here assigned to VOF$_2$.

Our calculated V−F stretching frequency matches better with the experimental one[17] than those calculated previously;[18] however, it remains in poor agreement and suggests a potential misassignment of the experimental data. We therefore compared frequencies of VOF and VOF$_2$ for our calculations with the experimental frequencies[17] for the peaks assigned to VOF, referred to hereafter as VOF$_x$ (see Table 7

Table 6. Structural Parameters for VO$_n$F$_m$ (Å for bond lengths, deg for angles)^a

	VOF$_3$		VOF$_2$	VOF		VO$_2$F
	present work	literature	present work	present work	literature	present work
V=O	1.59	1.575[12]	1.59	1.60	1.606,[18] 1.58[17]	1.61
V−F	1.71	1.73[12]	1.73	1.75	1.848,[18] 1.85[17]	1.74
O=V−F	108.3		116.1	123.0	144.4,[18] 167.4[17]	114.7
F−V−F	110.6	110.9[12]	127.7			
O−V−O						109.4

^{a} Experimental data in italics.

Table 7. Calculated and Literature Frequencies for VO$_n$F$_m$ (cm^{-1})^a

VOF$_3$		VOF$_2$	VOF		VOF$_x$	VO$_2$F
present work	literature	present work	present work	literature	literature	present work
1065	1058,[12] 1058,[8] 1057.8	1048	1013	1028.3,[18] 1132[17]	1028[17]	1033
807	806,[12] 806[8,7]	807	694	617,[18] 630[17]	807[17]	1017
710	722,[12] 722,[8] 721.5[7]	673	148	109.8,[18] 66.48[17]	668.7[17] (*)	731
289	308,[12] 308[7]	265				360
240	256,[12] 257.8[7]	192				237
186	205,[12] 204.3[7]	30				173

^{a} (*) indicates previously unassigned peak not considered by the authors. Experimental data in italics.

Table 8. Structural Parameters for VOCl$_3$, VOF$_3$, VOCl$_2$F, and VOClF$_2$ (Å for bond lengths and deg for angles)^a

	VOCl$_3$		VOCl$_2$F	VOClF$_2$	VOF$_3$	
	present work	literature	present work	present work	present work	literature
V=O	1.59	1.571,[12] 1.57,[14] 1.571[13]	1.59	1.59	1.59	1.575[12]
V−Cl	2.11	2.168,[12] 2.142,[14] 2.137[13]	2.11	2.11		
O=V−Cl	108.3	107.8[13]	108.1	108.0		
V−F			1.71	1.71	1.71	1.73[12]
O=V−F			108.7	108.3	108.3	

^{a} Experimental data in italics.

Table 9. Calculated and Literature Frequencies for VOCl$_3$, VOF$_3$, VOCl$_2$F, and VOClF$_2$ (cm^{-1})^a

VOCl$_3$	VOCl$_2$F	VOClF$_2$	VOF$_3$	VOF$_2$
present work	present work	present work	present work	present work
1046 (1035[8])	1055	1060	1065 (1058[8])	1048
502 (505[8])	759, 509	794, 731	807 (806[8,7])	807
397 (408[8])	435	475	710 (722[8])	673
243 (248[12])	270, 248	287, 266	289 (308[12])	265
161 (163[12])	184	207	240 (256[12])	192
126 (124.5[12])	158, 129	175, 154	186 (205[12])	30

^{a} Experimental data in italics. The VOF$_2$, VOCl$_2$F, and VOClF$_2$ frequencies correspond to unassigned peaks in the spectrum of ref 8 (see Figure 1).

Table 10. Structural Parameters for VO$_n$Br$_m$ (Å for bond lengths and deg for angles)^a

	VOBr$_3$		VOBr$_2$	VOBr	VO$_2$Br
	present work	literature	present work	present work	present work
V=O	1.59	1.572[12]	1.59	1.60	1.60
V−Br	2.25	2.331[12]	2.26	2.29	2.27
O=V−Br	108.3		116.5	120.5	113.5
Br−V−Br	110.6	111[12]	126.9		
O−V−O					109.2

^{a} Experimental data in italics.

Table 11. Calculated and Literature Frequencies for VO$_n$Br$_m$ (cm^{-1})^a

VOBr$_3$		VOBr$_2$	VOBr	VO$_2$Br
present work	literature	present work	present work	present work
1046	1025,[12] 1030,[8] 1025	1036	1013	1023
395	401,[12] 400,[8] 400[11]	422	320	1008
284	269,[12] 271[11]	280		394
210	212,[12] 212[11]	188		305
120	118,[12] 120[11]	76		168
81	84,[12] 83[11]	26	137	143

^{a} Experimental data in italics.

Table 12. Structural Parameters for VOCl$_3$, VOBr$_3$, VOBrCl$_2$, and VOBr$_2$Cl Molecules (Å for bond lengths and deg for angles)^a

	VOCl$_3$		VOBrCl$_2$	VOBr$_2$Cl	VOBr$_3$	
	present work	literature	present work	present work	present work	literature
V=O	1.59	1.571,[12] 1.57,[14] 1.571[13]	1.59	1.59	1.59	1.572[12]
V−Cl	2.11	2.168,[12] 2.142,[14] 2.137[13]	2.11	2.11		
O=V−Cl	108.3	107.8[13]	108.5	108.6		
V−Br			2.25	2.25	2.25	2.331[12]
O=V−Br			108.1	108.3	108.3	

^{a} Experimental data in italics.
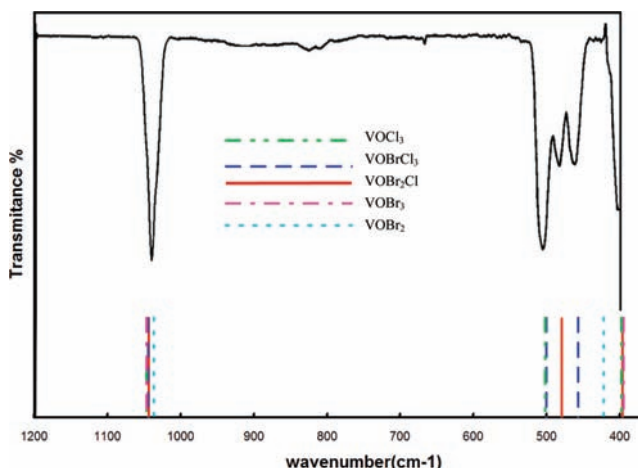
Figure 3. VOBr$_3$ FTIR absorption spectrum, modified from ref 8. Colored bars correspond to our calculated frequencies for various molecules, as given in the legend. Peaks at 457 and 479 cm^{-1} are assigned respectively to VOBrCl$_2$ and VOBr$_2$Cl. The shoulder at 422 cm^{-1} is assigned to VOBr$_2$.

and Figure 2). A much better match is obtained between VOF$_x$ and VOF$_2$ than between VOF$_x$ and VOF, particularly concerning the peak at 807 cm^{-1} (VOF$_3$ also has a mode at 807 cm^{-1}, but we assume, regarding its other very weak peak intensities, that it cannot alone explain the strong observed peak at 807 cm^{-1}). Moreover, the experimental spectrum for VOF$_x$ includes another peak at 668.7 cm^{-1} which was previously neglected.[17] This peak is in good agreement with our calculated frequency at 673 cm^{-1} for VOF$_2$, which has more vibrational frequencies than VOF. Since the process used to produce VOF could reasonably also produce other species such as VOF$_2$, and given the data above, we therefore reassign the experimental data

previously assigned to VOF to VOF$_2$. This is with the proviso that the spectra are somewhat noisy and the peak quite sharp, and without repeat experiments the possibility that the peak is an artifact cannot be completely excluded.

We note that this also suggests that the primary product of VOCl$_3$ reaction over NaF is VOF$_2$ rather than VOF$_3$ (Table 9 and Figure 1).

Table 13. Calculated and Literature Frequencies for VOCl$_3$, VOBr$_3$, VOBr$_2$, VOBrCl$_2$, and VOBr$_2$Cl (cm^{-1})^a

VOCl$_3$	VOBrCl$_2$	VOBr$_2$Cl	VOBrCl	VOBr$_3$	VOBr$_2$
present work	present work	present work	present work	present work	present work
1046 (*1035*[8])	1044	1043	1037	1046 (*1030*[8])	1036
502 (*505*[8])	500, 457	479, 397	489	395 (*400*[8])	422
397 (*408*[8])	328	319	334	284 (*271*[11])	280
243 (*248*[12])	242, 215	227, 205	182	210 (*212*[11])	188
161 (*163*[12])	148	133		120 (*120*[11])	76
126 (*124.5*[12])	115, 105	104, 87		81 (*83*[11])	26

^{a} Experimental data in italics. The VOBr$_2$, VOBrCl$_2$, and VOBr$_2$Cl calculated frequencies explain previously unassigned peaks in the VOBr$_3$ spectrum (see Figure 3).

Table 14. Structural Parameters for VO$_n$I$_m$ (Å for bond lengths and deg for angles)

	VOI$_3$		VOI$_2$	VOI	VO$_2$I
	present work	literature	present work	present work	present work
V=O	1.59	1.574[12]	1.59	1.60	1.61
V−I	2.47	2.332[12]	2.48	2.50	2.48
O=V−I	108.3		116.5	119.5	112.7
I−V−I	110.6	111[12]	127.1		
O−V−O					109.3

Table 15. Calculated and Literature Frequencies for VO$_n$I$_m$ (cm^{-1})^a

VOI$_3$		VOI$_2$	VOI	VO$_2$I
present work	literature	present work	present work	present work
1037	1022,[12] *1025*[8]	1034	1013	1020
331	333[12]	360	265	1006
216	207[12]	218		367
185	187[12]	173		270
87	91[12]	62		154
58	62[12]	31	121	133

^{a} Experimental value in italics.

As with VO$_2$Cl, VO$_2$F does not have frequencies that match any peaks in the experimental spectra.

3.3. Vanadium Oxobromides VOBr$_x$. We first consider VOBr$_3$, once again obtaining good structural agreement with

Table 16. Structural Parameters for VOCl$_3$, VOI$_3$, VOCl$_2$I, and VOClI$_2$ (Å for bond lengths, deg for angles)

	VOCl$_3$		VOCl$_2$I	VOClI$_2$	VOI$_3$	
	present work	literature	present work	present work	present work	literature
V=O	1.59	1.571,[12] *1.57*,[14] 1.571[13]	1.59	1.59	1.59	1.572[12]
V−Cl	2.11	2.168,[12] *2.142*,[14] 2.137[13]	2.12	2.12		
O=V−Cl	108.3	*107.8*[13]	108.8	109.4		
V−I			2.46	2.47	2.47	2.331[12]
O=V−I			107.3	107.8	108.3	

Table 17. Calculated and Literature Frequencies for VOCl$_3$, VOI$_3$, VOClI, VOCl$_2$I, and VOClI$_2$ (cm^{-1})^a

VOCl$_3$	VOCl$_2$I	VOClI$_2$	VOClI	VOI$_3$	VOI$_2$
present work	present work	present work	present work	present work	present work
1046 (*1035*[8])	1042	1039	1035	1037 (*1025*[8])	1034
502 (*505*[8])	497	487	475	331 (*333*[12])	360
397 (*408*[8])	442	381	290	216 (*207*[12])	218
243 (*248*[12])	313	323	182	185 (*187*[12])	173
161 (*163*[12])	240	275		87 (*91*[12])	62
126 (*124.5*[12])	195	197		58 (*62*[12])	31

^{a} Experimental data in italics.

theoretical[12] data from the literature where available (less than 0.08 Å difference for bond lengths, less than 0.4° difference for angles; see Tables 10 and 12).

Previously reported experimental FTIR data[8] for VOBr$_3$ (see Figure 3) show three unexplained peaks: a shoulder at the left of the V−Br stretching frequency around 400 cm^{-1} and two peaks to the right of the peak attributed to VOCl$_3$ (500 cm^{-1}). We propose the attribution of the shoulder peak to VOBr$_2$ (see Figure 3). The only other calculated frequency for VOBr$_2$ in the experimentally measured range is the V=O stretching frequency, which is almost identical to that of VOBr$_3$ (1030 cm^{-1}) and so will not be observable (see Tables 11 and 13). According to our calculations, the last two unassigned peaks correspond to the compounds VOBr$_2$Cl and VOBrCl$_2$ (see Table 13 and Figure 3). We also determined
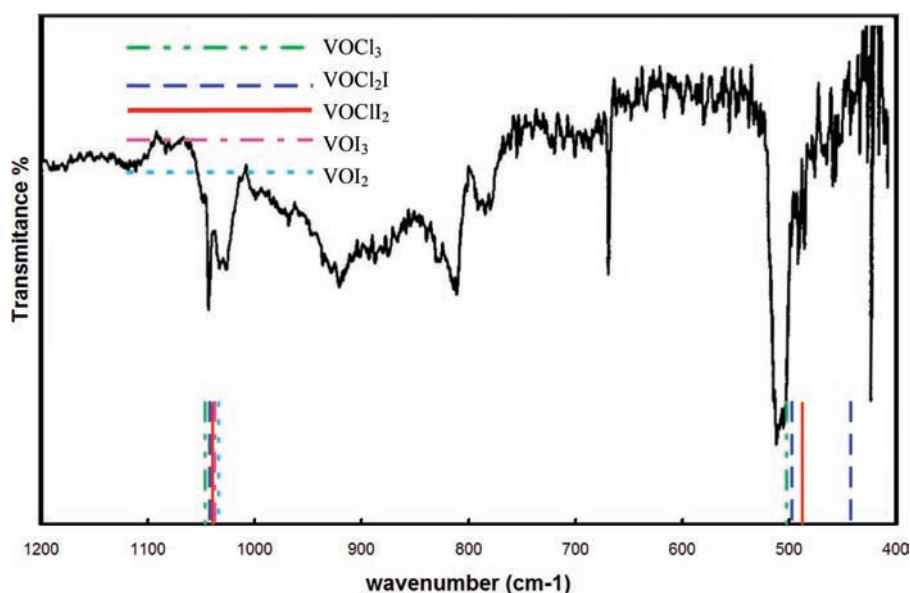

Figure 4. VOI$_3$ spectrum modified from ref 8. Colored bars correspond to calculated frequencies for various molecules, as given in the key. While the majority of observed unassigned peaks cannot be explained by our calculations, there appears evidence for the intermediates VOCl$_2$I, VOClI$_2$, and VOClI.

Table 18. Comparison of X−V−X Bond Angles between VOCl$_3$, VOF$_3$, VOBr$_3$, and VOI$_3$[a]

	VOCl$_3$		VOF$_3$		VOBr$_3$		VOI$_3$	
	present work	literature	present work	literature	present work	literature	present work	literature
X−V−X	110.6	110.9,[12] *111.3*,[14] *111*[13]	110.6	110.9[12]	110.6	111[12]	110.6	111[12]

[a] Experimental literature values in italics.

modes for VOBrCl, but they fall too close to other peaks for clear identification. Other calculated frequencies either fall outside the experimentally reported frequency range (under 400 cm^{-1}) or lie too near to VOCl$_3$ and VOBr$_3$ frequencies to be observed. Tables 10 and 11 also include new calculated data for VOBr and VO$_2$Br which have not previously been considered in the literature. With the exception of the V=O stretch modes, all of their modes fall below the experimentally reported frequency range 400−1200 cm^{-1} [8] (see Figure 3), thus precluding their identification.

3.4. Vanadium Oxoiodides VOI$_x$. Again for VOI$_3$, we obtain excellent structural agreement with literature data where available[12] (less than 0.14 Å difference for bond lengths, less than 0.4° difference for angles; see Tables 14 and 16). The experimental FTIR spectrum for VOI$_x$ in ref 8 (see Figure 4) contains many more peaks than for the other vanadium oxohalides, the vast majority of which were unassigned. We have calculated vibrational frequencies of VOI$_2$, VOI, and VO$_2$I, but as for VOI$_3$, they do not show frequencies in the experimentally reported range 400−1200 cm^{-1} (Table 15) apart from V=O stretch modes, which are too close to use for identification. We have also considered other possible contaminant species such as potassium compounds but did not clearly identify any species that accurately reproduced the experimental data. However, the calculated frequencies for VOCl$_2$I or VOClI$_2$ may explain some of the structure at the lower-frequency edge of the strong 505 cm^{-1} absorption due to VOCl$_3$ (see Table 17 and Figure 4).

4. Conclusions

We have studied a wide range of oxohalides of vanadium (VOX$_n$Y$_m$; X, Y = F, Cl, Br, I; n, m = 0−3, $(n + m) \leq 3$), giving generally excellent agreement between our calculated data and previous literature data where available. The results lead to the assignment and reassignment of many experimentally observed FTIR absorption peaks. Notably, we propose a reassignment of peaks for VOF[16,17] to VOF$_2$. The reported[8] spectrum for VOF$_3$ includes weak peaks and shoulders that we assign to VOCl$_2$F, VOClF$_2$, and VOF$_2$. The presence of VOCl$_2$ in samples of VOCl$_3$ thermally treated to produce VOCl cannot be excluded since its calculated absorption peaks lie in the shoulders of VOCl$_3$ peaks. We propose an inversion of attribution for two Cl

isotope peaks in the literature for VOCl$_3$.[15] The VOBr$_3$ spectrum includes three peaks that we assign to VOBr$_2$Cl and VOBrCl$_2$, and a shoulder we assign to VOBr$_2$. Finally, we are not able to definitively assign any of the many peaks observed in the VOI$_3$ spectrum to related VOI$_n$ or VOI$_n$Cl$_m$ species but suggest that some lower-frequency modes could be due to VOCl$_2$I and VOClI$_2$. We note that some of the remaining unassigned peaks in the spectra could be due to species hydrolyzing, forming hydrous pentoxides; however, these lie beyond the scope of the current study.

The lengthening of the V−X bond from X = F to I appears to be due to the size of the halogen atoms. Steric hindrance between the halogen atoms is unlikely given the X−V−X angle for VOX$_3$ (Table 18), which remains practically unchanged from Cl to I.

Given the new frequency assignments, a more complete interpretation of vanadium oxohalide formation via online heating of halide salts is now possible, following clearly a trend of decreasing the V−X bond strength (and increasing bond length) as X moves down the periodic table from F to I.

VOF$_3$ is a very stable molecule, and V−F bonds seem hard to break. Indeed, dissociation processes lead to VOF$_2$ rather than to VOF. While conversion of VOCl$_3$ to VOF$_3$ does not have 100% yield, the byproducts (VOCl$_2$F and VOClF$_2$) are only observed in small quantities.

VOCl$_3$ is less stable, and V−Cl bonds are easier to break. Dissociation thus gives experimentally VOCl, although VOCl$_2$ byproduct production cannot be excluded.

VOBr$_3$ has much weaker V−Br bonds. In this case, the production of VOBr$_3$ by cracking VOCl$_3$ results in large quantities of stable VOBr$_x$Cl$_{3-x}$ (x = 1, 2) intermediates, as well as spontaneous formation of some VOBr$_2$.

VOI$_3$ is certainly the least stable of the four. Its existence cannot be definitely confirmed with the available literature data,[8] and observed peaks may be due to other species, possibly VOClI$_2$ and VOCl$_2$I. Experimental data at lower IR frequencies are needed to confirm these assignments.